Journal of Solid State Chemistry 183 (2010) 969–974

Contents lists available at ScienceDirect

Journal of Solid State Chemistry

journal homepage: www.elsevier.com/locate/jssc

Carbon/λ-MnO_2 composites for supercapacitor electrodes

A. Malak-Polaczyk [a,b,*], C. Matei-Ghimbeu [b], C. Vix-Guterl [b], E. Frackowiak [a]

[a] Institute of Chemistry and Technical Electrochemistry, Poznan University of Technology, Piotrowo 3, 60-695 Poznan, Poland
[b] Institut de Sciences des Matériaux de Mulhouse, CNRS LRC 7228, 15 Rue Starcky, 68057 Mulhouse, France

ARTICLE INFO

Article history:
Received 3 November 2009
Received in revised form
16 February 2010
Accepted 20 February 2010
Available online 26 February 2010

Keywords:
Manganese oxide
Pseudocapacitance
Supercapacitor
Activated carbon

ABSTRACT

In the present work a composite of carbon with λ-MnO_2 have been synthesized by a simple two-step route. In the first step, to obtain $LiMn_2O_4$/carbon material, mesoporous activated carbon was impregnated with the solution of precursor metal salts and heated subsequently. As-prepared materials were acid treated which resulted in the formation of λ-MnO_2/carbon. Physical properties, structure and specific surface area of electrode materials were studied by TEM, X-ray diffraction and nitrogen sorption measurements. Voltammetry cycling, galvanostatic charge/discharge and impedance spectroscopy measurements performed in two- and three-electrode cells have been applied in order to measure electrochemical parameters. TEM images confirmed well dispersed λ-MnO_2 particles on the surface of carbon material. The carbon in the composite plays an important role as the surface area enhancing component and a support of pseudocapacitive material. Furthermore, the through-connected porosity serves as a continuous pathway for electrolyte transport. A synergetic effect of the porous carbon framework and of the redox properties of the λ-MnO_2 is at the origin of improvement of specific capacitance values which has been observed for composites after delithiation.

1. Introduction

It is commonly known, that manganese dioxide, due to its low cost, environmentally friendly nature and high theoretical capacitance, is a promising electrode material for electrochemical capacitors [1–7]. Till present different techniques have been employed to prepare MnO_2 powders or films with controlled properties (porosity, particle size, crystal structure, etc.) in order to improve its electrochemical performances. They include electrodeposition or chemical synthesis of oxides with porous morphology [8,9], reduction in particle size, preparing composites with carbon nanotubes (CNTs) [10], carbon materials [11–13], other metal oxides [14,15] and conducting polymers [16]. All these attempts have shown some improvement in maximizing the utilization of hydrous MnO_2, but still, substantial improvements have to be made for its successful commercialization.

The enhancement of electrical properties can also be achieved by immersing lithium manganese oxide powder in sulphuric acid in order to extract lithium ions from the intercalated compound. It has been reported [17] that treatment of the spinel-type material $LiMn_2O_4$ with aqueous acid solution leads to conversion of the $LiMn_2O_4$ to a defected MnO_2 phase, while preserving the structural framework of the $LiMn_2O_4$. Mechanism of the removal of lithium from $LiMn_2O_4$ has been studied previously [18] and involves dissolution of lithium oxide and surface disproportionation reaction of two trivalent manganese ions.

As it is well known, the $LiMn_2O_4$ is one of the mostly used cathode material in Li-ion batteries and for this reason the subject of many papers [19,20]. On the contrary, concerning application of $LiMn_2O_4$ as an electrode in a hybrid supercapacitor only few reports have been published [21,22]. We showed in a previous paper that combination of λ-MnO_2 as positive and activated carbon as negative electrode led to an asymmetric capacitor able to work within extended potential window limited to 2.0 V for cycling [23]. However, because an effective utilization of pseudocapacitive material for the ion insertion is limited only to the outer surface of the electrode, the decrease of specific capacitance values at higher current densities has been observed for pure λ-MnO_2 electrode. In this paper an attempt is made to overcome the above mentioned disadvantage by synthesizing a composite electrode, consisting of carbon and λ-MnO_2, where λ-MnO_2 is a product of lithium extraction from lithium manganese oxide spinel using the acid treatment. Introducing λ-MnO_2 into the porous, high surface area and electronically conducting carbon material should optimize the electrochemical performance and enhance effective utilization of λ-MnO_2.

* Corresponding author at: Institute of Chemistry and Technical Electrochemistry, Poznan University of Technology, Piotrowo 3, 60-695 Poznan, Poland.
Fax: +48 61 665 37 91.
E-mail addresses: agnieszka-malak@wp.pl, aga.polaczyk@wp.pl (A. Malak-Polaczyk).

0022-4596/$ - see front matter © 2010 Elsevier Inc. All rights reserved.
doi:10.1016/j.jssc.2010.02.015

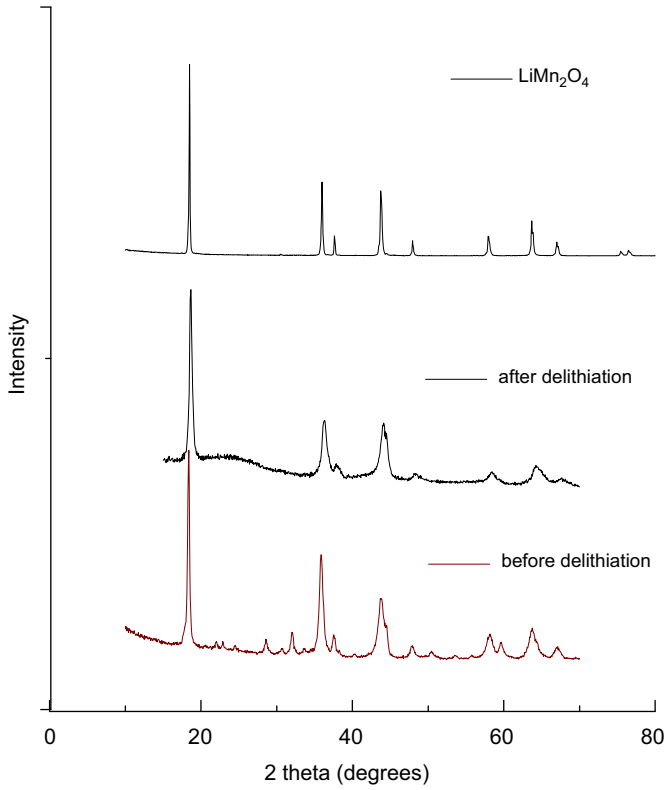

Fig. 1. XRD patterns of composite CA before and after delithiation.

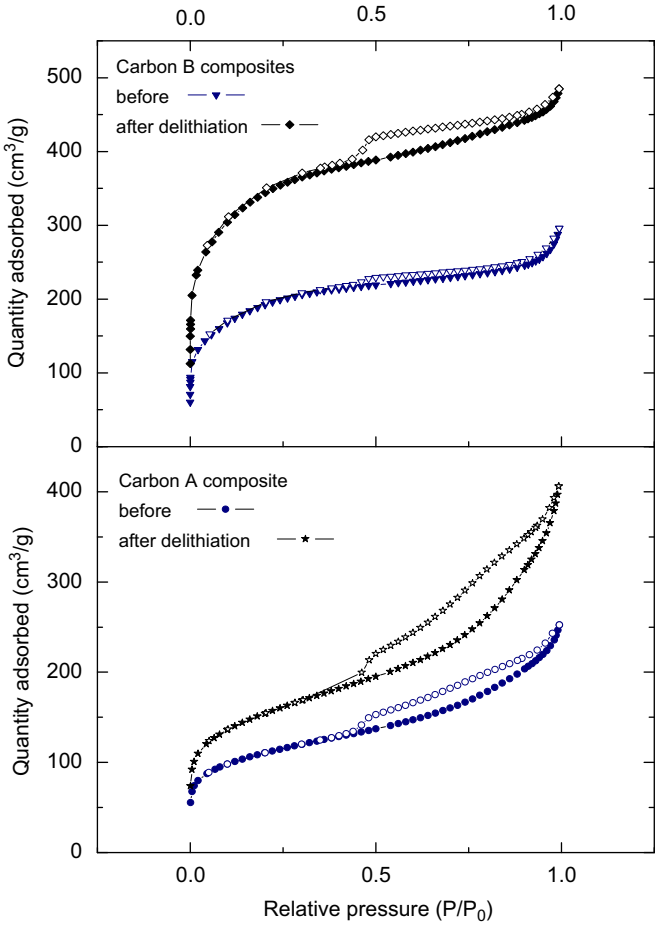

Fig. 2. Nitrogen adsorption isotherms for composites CA and CB.

2. Experimental section

2.1. Material preparation

Two different activated carbon materials were supplied by NORIT: CGRAN-granular activated carbon, produced by chemical activation using the phosphoric acid process and A SUPRA EUR which is a steam activated carbon. These materials are designated as CA and CB, respectively. Sulphuric acid 95%, lithium nitrate and manganese nitrate were commercially available reagents (p.a.) from Aldrich and Fluka.

In the first step $LiMn_2O_4$/carbon composite was obtained by the impregnation of mesoporous activated carbon (2 g) with 10 ml of a highly concentrated solution (4 M in distilled water) of $LiNO_3$ and $Mn(NO_3)_2 \cdot 4H_2O$ with the molar ratio Li:Mn equal to 1:1.

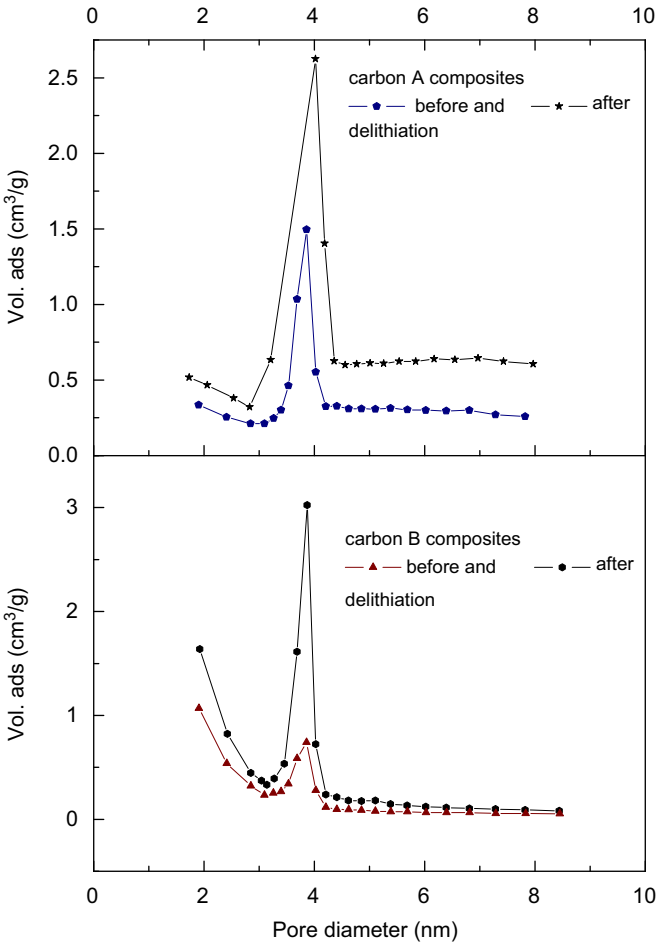

Fig. 3. BJH pore size distribution for composites CA and CB.

Table 1
Specific surface area and total pore volume calculated from nitrogen sorption isotherm for carbon and composite materials.

	S_{BET} ($m^2\,g^{-1}$)	V_t ($cm^3\,g^{-1}$)
Carbon A	1350	0.65
$LiMn_2O_4$/CA	373	0.34
λ-MnO_2/CA	523	0.53
Carbon B	1633	0.88
$LiMn_2O_4$/CB	647	0.41
λ-MnO_2/CB	1144	0.7

Prior to the impregnation the carbon was outgassed in air for one night at 100 °C to remove the possible water traces. The impregnated carbon was shaked for 1 h, then filtered and dried with filter paper. Subsequently thermal treatment was done in synthetic air (10 l/h) for 1 h at different temperatures ranging 300–800 °C using a heating rate of 5 °C/min.

To obtain the λ-MnO_2 compounds, the $LiMn_2O_4$/carbon powder was treated with diluted aqueous solution of sulphuric acid and stirred for 24 h. After that, the solution was filtered and deposit washed several times with distilled water and dried in air at 100 °C. The final product is designated λ-MnO_2/carbon.

In the present work, for further and more detailed investigation, two composites with the most interesting and well defined properties (one representative of each carbon) have been selected.

2.2. Physical measurements

The textural properties of the materials were determined by nitrogen adsorption at 77 K using a Micromeritrics ASAP2020 set-up. The specific surface area was evaluated according to the BET equation in the region 0.05–0.3 of a relative pressure. The total pore volume was determined at a relative pressure $P/P_0=0.95$ while the pore sizes and pore size distributions were calculated by the BJH method from the desorption branches.

The crystallinity and the structure of the samples were evaluated by X-ray diffraction technique. XRD analysis of each sample was carried out using Philips X'pert MPD diffractometer equipped with a Cu anode to generate Cu$K\alpha$ radiation ($\lambda=1.5406$ Å). Each diffraction pattern was collected in the 2θ range 15–70° with the step size of 0.05° and a count time of 5.0 s per step.

2.3. Electrochemical characterization

The capacitor electrodes for evaluating the electrochemical properties were formed as pellets consisting of 85% composite material, 5% acetylene black and 10% binder (PVDF, Kynar Flex 2801). These pellets were 10 mm in diameter and 0.20 mm ($\pm$0.02 mm) in thickness and were prepared under pressure of 10 MPa. The typical mass of the electrode material ranged 11.0–12.5 mg. Symmetric supercapacitors were operating in 1 mol L^{-1} Na_2SO_4 electrolytic solution. All experiments were carried out at room temperature.

The capacitance values were estimated in two-electrode Swagelok® system by galvanostatic charge/discharge and cyclic voltammetry with different scan rates using VMP3 (Biologic–France). In the case of a three-electrode cell, Hg/Hg_2SO_4 system was used as a reference. The capacitance values of material were calculated per mass of active material in one electrode. The specific capacitance has been evaluated using the formula $C=I\Delta t/(m\Delta V)$, where i is the current used for discharge, Δt is the time elapsed for the discharge, m is the mass of the active electrode and ΔV is the voltage range of the discharge.

3. Results and discussion

Thermal treatment in the wide range of temperatures and different times allowed to optimize conditions for both carbon

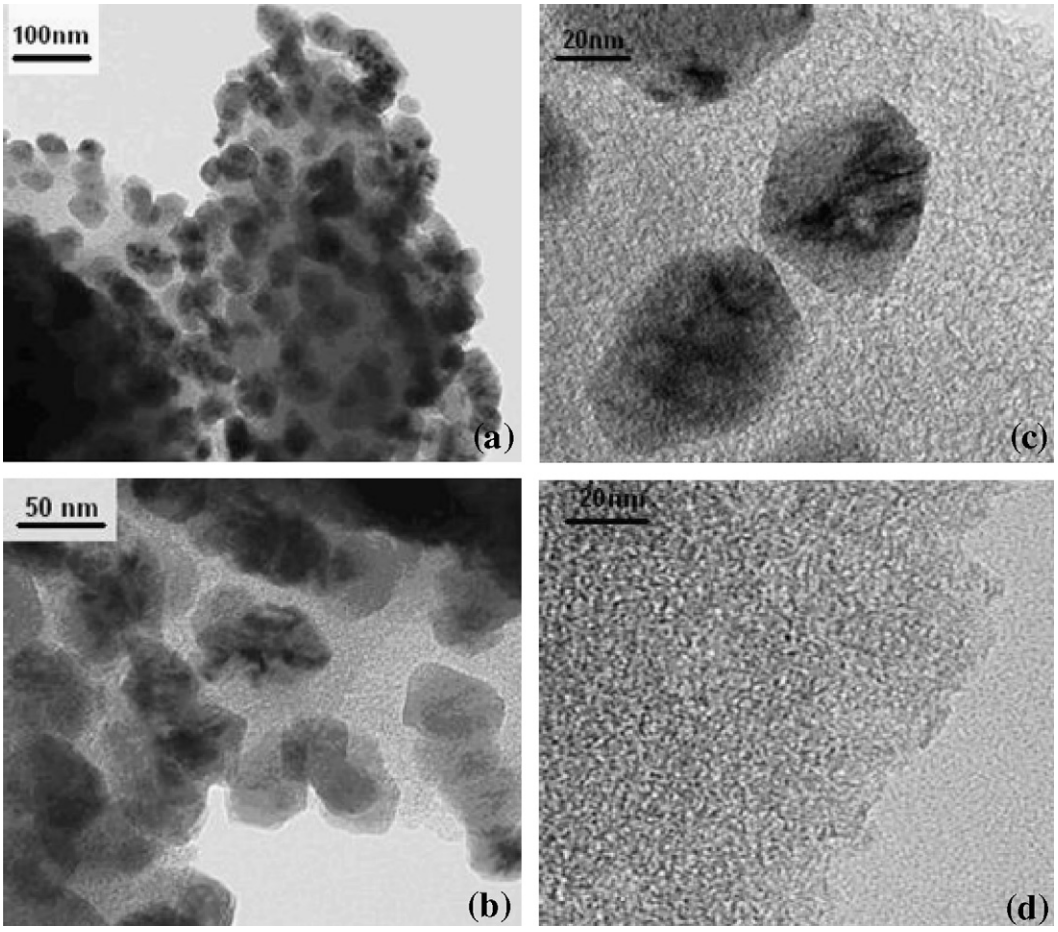

Fig. 4. TEM images of composite CB (a), (b), (c) and carbon B (d).

composite materials, which are 600 ± 3 and 300 ± 3 °C for CA and CB, respectively. Such significant difference can be explained by the preparation method of each activated carbon.

Mechanism of the removal of lithium from $LiMn_2O_4$ has been studied previously and the proposed reaction is as follows: [17]

$$2Li(Mn^{3+}Mn^{4+})O_4 + 4H^+ \rightarrow 3\lambda - MnO_2 + Mn^{2+}_{solution} + 2Li^+ + 2H_2O$$

The mechanism involves dissolution of lithium oxide and surface disproportionation reaction of two trivalent manganese ions. $LiMn_2O_4$ spinel has a cubic close-packed structure. Half of the octahedral sites of the lattice is occupied by manganese ions and one eighth of the tetrahedral sites by lithium ions. In stoichiometric spinel, the manganese ions coexist in two valence states Mn^{3+} and Mn^{4+} in equal proportions, hence the chemical formula can be written as $Li(Mn^{3+}Mn^{4+})O_4$ [20]. It has been shown that treatment of the spinel-type material $LiMn_2O_4$ with aqueous acid leads to conversion of the $LiMn_2O_4$ to nearly pure MnO_2, while preserving the structural framework of the $LiMn_2O_4$. After treatment most of the lithium ions are removed from the tetrahedral sites but the structural framework of spinel is preserved.

The structure evaluated by XRD proved the formation of crystalline $LiMn_2O_4$ but also the presence of small quantities of Mn_2O_3. The results of X-ray diffraction measurements are given in Fig. 1. The diffraction peaks of composite are well matched to the pure cubic spinel structure (JCPDS 35-0782). λ-MnO_2/carbon has the same pattern concerning relative line position, while the peaks shift slightly towards lower d values (higher 2θ). This indicates that the spinel structure is maintained after removal of lithium ions. All values are with good agreement with the reported data for pure phase of λ-MnO_2 (JCPDS no. 44-0992). From the pattern obtained after delithiation it can be seen, that acid treatment also removed Mn_2O_3 impurities. These can be explained by acid digestion of lower manganese oxides such as Mn_2O_3, Mn_3O_4 which occurs in H_2SO_4 solution [24]. The digestion process of Mn_2O_3 can be divided in two steps: (a) dissolution of the Mn_2O_3 into soluble Mn^{3+} species in the electrolyte:

$$Mn_2O_3 + 6H^+ \leftrightarrow 2Mn^{3+} + 3H_2O$$

and (b) the disproportionation of soluble Mn^{3+} into manganese dioxide and soluble Mn^{2+},

$$2Mn^{3+} + 2H_2O \leftrightarrow MnO_2 + Mn^{2+} + 4H^+$$

overall: $Mn_2O_3 + 2H^+ \leftrightarrow MnO_2 + Mn^{2+} + H_2O$

The dissolution step is based on the stability of soluble Mn^{3+} in low pH solution in the Pourbaix diagram. It has been shown [25] that there is a short induction period before the transformation into Mn_2O begins. The origin of this induction period is probably a saturation of the electrolyte with Mn^{3+} as a result of Mn_2O_3 dissolution before disproportionation occurs.

The results of nitrogen sorption measurements are presented in Figs. 2 and 3. The calculated values of specific surface and total pore volume are listed in Table 1.

The highest specific surface area of material before delithiation ($647\ m^2/g$) was determined for the composite prepared with CB at 300 °C which contained 80% of residual carbon.

Increase of both specific surface area and pore volume for the material after acid treatment is believed to be caused by extraction of lithium ions from spinel. Furthermore, the dissolution of manganese induced by acid treatment also occurs which results in oxidizing a part of Mn^{3+} ions to higher oxidation state Mn^{4+} and formation of a λ-MnO_2/CB composite with a better developed porosity ($1144\ m^2/g$). Increase of pore volume (Fig. 3) can also be explained by the dissolution of lower manganese oxides impurities which, in $LiMn_2O_4$/carbon composite, may have filled in or blocked some of the pores.

Fig. 4(a–c) shows the TEM images of the as-received λ-MnO_2/carbon composite, from which formation of oxide particles seems to be apparent, especially when compared with the image of pure carbon (Fig. 4d). These pictures suggest that the particles are separated and dispersed within activated carbon. Existence of Mn and O has been confirmed by energy-dispersive analysis of the X-ray spectrum which also indicated presence of residual carbon (50–80%).

Electrochemical properties of synthesized composites have been evaluated in two- and three-electrode systems. In Fig. 5 comparison of cyclic voltammograms of carbon material, composite with spinel and with λ-MnO_2 for carbons A and B (Fig. 5 (a) and (b), respectively) are presented. Improvement of capacitance can be observed for composites with $LiMn_2O_4$ and more evident for λ-MnO_2/CA and comparing to the initial material. The capacitance determined in $1\ mol\ L^{-1}$ Na_2SO_4 for the composite is of the order of $80\ Fg^{-1}$ (λ-MnO_2/CA) and $110\ Fg^{-1}$ (λ-MnO_2/CB), whereas in the same conditions the capacitance value is 5 and $60\ Fg^{-1}$ for pristines CA and CB, respectively. Since the λ-MnO_2/carbon composite has a BET specific surface area ($523\ m^2g^{-1}$ λ-MnO_2/CA, $1144\ m^2g^{-1}$ λ-MnO_2/CB) lower than the initial carbon material (1350 CA and $1633\ m^2g^{-1}$ CB), the additional contribution to the capacitance is due to the pseudofaradic charge transfer reactions, in both cases.

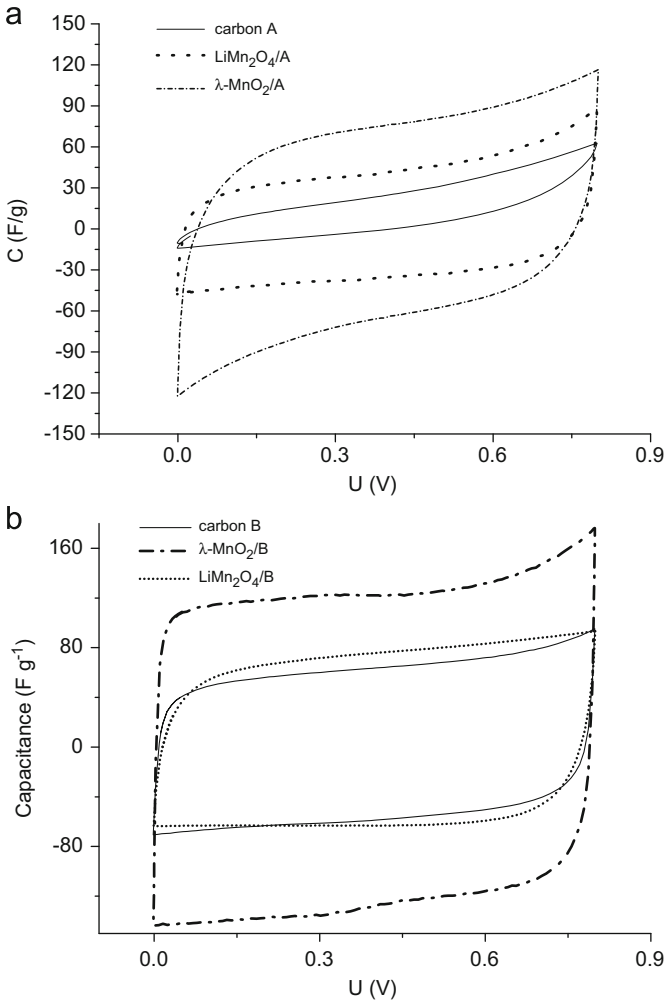

Fig. 5. Comparison of capacitance characteristics for initial carbon and synthesized composites for CA (a) and CB (b) in $1\ mol\ L^{-1}$ Na_2SO_4 solution.

Table 2
Capacitance values estimated at different current loads for carbon materials and synthesised composites.

Material	Capacitance (Fg^{-1})				
	50 (mAg^{-1})	100 (mAg^{-1})	200 (mAg^{-1})	500 (mAg^{-1})	1000 (mAg^{-1})
Carbon A	5	2	1.1	0.5	–
$LiMn_2O_4$/CA	31	28	25	15	2
λ-MnO_2/CA	85	75	60	40	30
Carbon B	60	52	45	30	15
$LiMn_2O_4$/CB	64	61	57	51	48
λ-MnO_2/CB	120	115	111	90	82

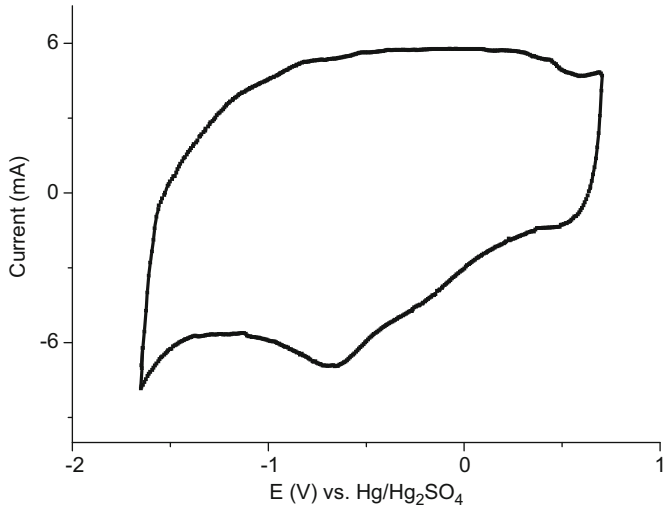

Fig. 6. Cyclic voltammogram for the λ-MnO_2/CB electrode within potential range from -1.65 to $+0.6$ V vs. Hg/Hg_2SO_4 at a scan rate of 5 mV s^{-1} in 1 mol L^{-1} Na_2SO_4 solution.

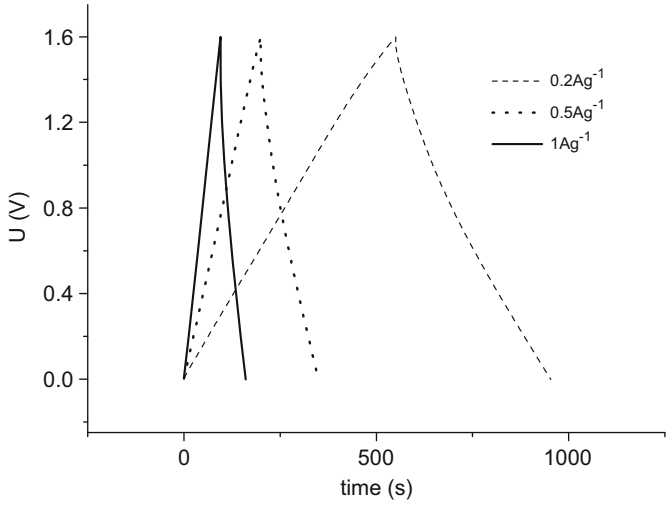

Fig. 7. Galvanostatic charge/discharge curves of symmetric capacitor at different current densities in 1 mol L^{-1} Na_2SO_4 aqueous solution.

It is worth noting that the electrochemical performance of such MnO_2/carbon structures is largely affected by the morphology and distribution of the MnO_2 phase but the origin and texture of the carbon framework have to be considered. Significant difference between electrochemical performances of these two activated carbon materials can be an evidence for this suggestion.

Two-electrode cells built from the λ-MnO_2/CB composite pellets in 1 mol L^{-1} Na_2SO_4 show the typical electrochemical characteristics of a capacitor (Fig. 5b). The voltammograms have nearly rectangular shape, which indicates a quick dynamic of charge propagation with this kind of composite. Galvanostatic charge/discharge measurements at a different current density were applied to estimate electrochemical properties. Specific capacitance calculated from charge/discharge curves is listed in Table 2.

Another advantage of this new type of electrode is its ability to work within extended potential window (Fig. 6). The two components are materials with different charge-storage mechanism. In the case of carbon the charges are stored in the electrode/electrolyte interface while for λ-MnO_2 the faradaic reaction rather than double layer charging is responsible for charge storage. Consequently they work in different potential ranges allowing the working potential of the composite to be extended. The challenge is to obtain composite with properly chosen amount of λ-MnO_2 incorporated, and thus making the best use of the active material.

Fig. 7 shows the galvanostatic charge/discharge plots of the symmetric capacitor at various current densities in 1 M Na_2SO_4 solution working in extended potential window. The charge and discharge curves are basically symmetric, however, the specific gravimetric capacitance fades with discharge current density. The reason for such behaviour is that the redox reaction takes place only on the surface area of the material under high current.

Additionally electrochemical impedance spectra (EIS) performed in the frequency range 100 kHz–1 MHz confirms decrease of resistance for material with carbon (not presented here).

4. Conclusions

In present work a composite of carbon with λ-MnO_2 has been synthesized, where λ-MnO_2 is a product of lithium extraction from lithium manganese oxide spinel using the acid treatment. To integrate λ-MnO_2 into the carbon, a $LiMn_2O_4$/carbon composite was obtained by the impregnation of mesoporous activated carbon with the precursors such as metal salts solution, followed by a thermal treatment and immersing in sulphuric acid in order to extract Li-ions.

It has been proved that introducing proper amount of λ-MnO_2 into the porous, high surface area carbon material allows to enhance effective utilization of λ-MnO_2. A synergetic effect of the porous carbon framework and the redox properties of the λ-MnO_2 is at the origin of improvement of specific capacitance values which has been observed for composites after delithiation. Additionally, this work promotes a system with aqueous electrolyte, which is cheaper and, what is more important, much more environment friendly.

References

[1] Y.U. Jeong, A. Manthiram, J. Electrochem. Soc. 149 (2002) A1419–A1422.
[2] J. Wei, N. Nagarajan, I. Zhitomirsky, J. Mater. Process. Technol. 186 (2007) 356–361.

[3] S.C. Pang, M.A. Anderson, J. Mater. Res. 15 (2000) 2096–2106.
[4] M. Toupin, T. Brousse, D. Bélanger, Chem. Mater. 14 (2002) 3946–3952.
[5] J. Jiang, A. Kucernak, Electrochim. Acta 47 (2002) 2381–2386.
[6] H.Y. Lee, V. Manivannan, J.B. Goodenough, C.R. Acad. Sci. Paris Chim. 2 (1999) 565–577.
[7] R.N. Reddy, R.G. Reddy, J. Power Sour. 124 (2003) 330–337.
[8] J.K. Chang, Yi.L. Chen, W.T. Tsai, J. Power Sour. 135 (2004) 344–353.
[9] S.C. Pang, M.A. Anderson, T.W. Chapman, J. Electrochem. Soc. 147 (2000) 444–450.
[10] E. Raymundo-Pinero, V. Khomenko, E. Frackowiak, F. Beguin, J. Electrochem. Soc. 152 (2005) A229–A235.
[11] Ch. Wan, K. Azumi, H. Konno, Electrochim. Acta 52 (2007) 3061–3066.
[12] M. Wu, G.A. Snook, G.Z. Chen, D.J. Fray, Electrochem. Commun. 6 (2004) 499–504.
[13] J.K. Chang, C.T. Lin, W.T. Tsai, Electrochem. Commun. 6 (2004) 666–671.
[14] D.J. Jones, E. Wortham, J. Rozière, F. Favier, J.L. Pascal, L. Monconduit, J. Phys. Chem. Solids 65 (2004) 235–239.
[15] H. Kim, B.N. Popov, J. Electrochem. Soc. 150 (2003) D56–D62.
[16] L.J. Suna, X.X. Liu, K.K. Laub, L. Chena, W.M. Gua, Electrochim. Acta 53 (2008) 3036–3042.
[17] J.C. Hunter, J. Solid State Chem. 39 (1981) 142–147.
[18] B. Ammundsen, P.B. Aitchison, G.R. Burns, D.J. Jones, J. Rozière, Solid State Ionics 97 (1997) 269–276.
[19] J.M. Tarascon, D. Guyomard, J. Electrochem. Soc. 138 (1991) 2864–2868.
[20] B. Goodenough, A. Manthiram, B. Wnetrzewski, J. Power Sour. 43 (1993) 269–275.
[21] Y.G. Wang, Y.Y. Xia, Electrochem. Commun. 7 (2005) 1138–1142.
[22] S.B. Ma, K.W. Nam, W.S. Yoon, X.Q. Yang, K.Y. Ahn, K.H. Oh, K.B. Kim, Electrochem. Commun. 9 (2007) 2807–2811.
[23] A. Malak, K. Fic, G. Lota, C. Vix-Guterl, E. Frackowiak, J. Solid State Electrochem. 14 (2010) 811–816.
[24] D.K. Walanda, G.A. Lawrance, S.W. Donne, J. Power Sour. 139 (2005) 325–341.
[25] D.K. Walanda, G.A. Lawrance, S.W. Donne, J. Solid State Chem. 182 (2009) 1336–1342.